A Sequential Autohydrolysis-Ionic Liquid Fractionation Process for High Quality Lignin Production

Jing Wang [a,b], Kalavathy Rajan [a], Aparna Annamraju [a,c], Stephen C. Chmely [d], Sai Venkatesh Pingali [e], Danielle Julie Carrier [b], and Nicole Labbé [a,c*]

Author affiliations

[a] Center of Renewable Carbon, The University of Tennessee Institute of Agriculture, Knoxville, TN 37996, USA.

[b] Department of Biosystems Engineering and Soil Science, The University of Tennessee Institute of Agriculture, Knoxville, TN 37996, USA.

[c] Department of Forestry, Wildlife and Fisheries, The University of Tennessee Institute of Agriculture, Knoxville, TN 37996, USA.

[d] Department of Agricultural and Biological Engineering, Pennsylvania State University, 225 Ag Engineering Building, Shortlidge Road, University Park, PA 16802, USA.

[e] Neutron Scattering Division, Oak Ridge National Laboratory, P. O. Box 2008, Oak Ridge, TN 37831, USA.

*** Corresponding author contact information**: Center for Renewable Carbon, The University of Tennessee, 2506 Jacob Drive, Knoxville, TN 37996, USA. **Email:** nlabbe@utk.edu. **Phone:** +1 (865) 946-1126.

Abstract

In this study, we propose a complete biomass fractionation strategy where all three major biopolymers, namely cellulose, hemicellulose and lignin, are separated with higher efficiency and purity. Sequential treatment of hybrid poplar wood using autohydrolysis (160 °C, 60 min) and 1-ethyl-3-methylimidazolium acetate activation (60 °C, 3 h) resulted in significantly improved enzymatic saccharification and fractionated 85% cellulose and 67% hemicellulose. The resulting solid fraction contained 90 % (w/w) lignin, which was equal to 71% yield based on the original biomass composition. The proposed two-step pretreatment process improved lignin yield by 77% and 23% compared to single-stage ionic liquid activation or autohydrolysis, respectively. Structural characterization by 2D nuclear magnetic resonance spectroscopy and small-angle neutron scattering revealed that the isolated lignin sustained minimal modifications to inter-unit linkages, and exhibited high thermotolerance as well as unique functionality, thereby highlighting the benefits of this process for lignin fractionation.

Keywords: Autohydrolysis; [C_2mim][OAc]; ionic liquid activation; enzymatic saccharification; lignin; biomass fractionation; hybrid poplar; 2D-HSQC NMR; SANS.

1. Introduction

Lignocellulosic biomass has been investigated as a renewable resource to generate fuels, chemicals, and other bio-products. However, the complex structural and chemical properties of lignocellulosic biomass render it highly resistant to fractionation via biochemical, physico-chemical and thermo-mechanical platforms.[1] To overcome this recalcitrance, a variety of pretreatment processes have been developed that target cellulose crystallinity, biomass porosity and dissolution of matrix polysaccharides.[2] Autohydrolysis pretreatment, for example, is reported to improve the conversion of cellulose into fermentable sugars by 42 to 86%,[3, 4] where the biomass recalcitrance is reduced via partial hemicellulose removal. However, lignin and hemicellulose that form majority of the plant cell wall are not effectively fractionated and recovered during these processes resulting in large amounts of low value by-products. A desirable biomass conversion process should facilitate maximization of biorefinery outputs, while minimizing its environmental impact. To achieve this goal, horizontal integration of biorefineries has been proposed, which follows the model of petrochemical industries and integrates low value-large volume fuel production with the generation of high value chemicals from the primary components of lignocellulosic feedstock.[5] Novel processes that satisfy integrated biorefinery requirements must demonstrate effectiveness for selective separation of each lignocellulosic component, while providing high purity of the isolated fractions. Ionic liquid (IL) processes have received significant attention as a potential technology to meet these requirements.

Ionic liquids (ILs) are molten salts with low melting points, high boiling points, and remain in liquid state at room temperature.[6] Continued research has brought down the bulk chemical costs ($1.24/kg) of ILs, and when coupled with efficient solvent recycling design, IL-based processing has immense potential for sustainable conversion of lignocellulosic

biomass.[7] The majority of IL processes have been proposed at high temperatures to either pretreat or fractionate lignocellulosic biomass and improve its ability to release fermentable sugars.[8, 9] The removal of lignin and hemicellulose, which generates a cellulose-rich fraction, contributes to the rapid dissolution of biomass at high pretreatment temperatures, especially above 150 °C.[10] Interestingly, pretreatment of wheat straw with 1-ethyl-3-methylimidazolium acetate at 140 °C was reported to generate high purity fractions of cellulose, hemicellulose, and lignin, however the lignin recovery was less than 50%.[11] Reducing the IL pretreatment duration from 6 to 2 h, at 140 °C, resulted in higher lignin recovery of 90% from sugarcane bagasse, however the total carbohydrate recovery was only 54%.[12] Milder IL pretreatment conditions of 60 °C, for 1 to 72 h, was reported to significantly reduce the recalcitrance of lignocellulosic biomass, while simultaneously minimizing the degradation of its major biopolymers.[13] This indicates that, 'mild' IL pretreatment has greater potential for efficient fractionation of lignocellulosic biomass.

Frequently, the use of IL as pretreatment resulted in lignin and hemicellulose fractions being underutilized, mostly due to degradation and distribution in other product streams.[10, 14] For example, in a one-pot IL saccharification system, which liberated 81.2% of glucose and 87.4% of xylose in 72 h, a part of the lignin was depolymerized and dissolved in the liquid stream, whereas the rest ended up in the solid stream with <70% purity.[14] More recent methods developed for the separation of lignocellulosic biomass into three distinct lignin, cellulose, and hemicellulose-rich fractions still had drawbacks, specifically inefficient recovery of highly pure lignin.[15, 16] IL-dissolution of biomass was reported to recover 70-80% of the carbohydrates, but only about 10-18% of lignin.[16] To maximize lignin recovery from pretreated residues, a sequential resin adsorption and supercritical CO_2 extraction was proposed, however the process only yielded 42% of

lignin.[17] High-purity lignin with preserved functionality has valuable applications in the development of platform chemicals and bio-based materials, but most of the available fractionation techniques result in the degradation of native lignin structure, reduction of molecular weight, increase in polydispersity, and decrease in functionality.[18] Hence, a direct and complete fractionation of biomass into individual biopolymers with high purity and yield remains a challenge. Integrated technologies could enhance the economic viability of biorefineries by producing three valuable co-product streams from lignocellulosic biomass and IL-based routes may rise to the challenge.

To our knowledge, there is potential for improving the fractionation yields by deploying ILs. The incremental increase in yield and purity, however small, is still valuable for enhancing the economic feasibility and sustainability of biorefineries. The main goal of this study is to develop a strategy to sequentially fractionate hybrid poplar (HP) biomass into cellulose, hemicellulose and lignin with high yield and purity. A two-step autohydrolysis and IL-activation pretreatment is proposed and evaluated with respect to its effectiveness on biomass fractionation. Powder X-ray diffractometry (XRD) is used to assess cellulose structural changes and subsequent enzymatic saccharification is performed to evaluate the recalcitrance of the treated biomass. Finally, the isolated lignin fraction (IL-lignin) is characterized by wet chemistry, differential scanning calorimetry (DSC), small angle neutron scattering (SANS), and 2D-HSQC (heteronuclear single quantum coherence) NMR spectroscopy to assess its purity and changes in physico-chemical properties.

2. Experimental Section

2.1. Materials and Chemicals

Hybrid poplar (*Populus deltoides*) (HP) wood was obtained from the Center for Renewable Carbon (University of Tennessee, Knoxville, TN). The biomass was air-dried

and chipped into less than 1 cm^3 particle size. The ionic liquid, ≥ 95% 1-ethyl-3-methylimidazolium acetate or [C_2mim][OAc], was purchased from Iolitec Inc. (Tuscaloosa, AL) and used without further purification. Dimethyl sulfoxide-d_6 (99.9%), pyridine-d_5 (99.5%), acetic acid-d_4 (≥ 95%) were purchased from Cambridge Isotope Laboratories (Tewksbury, MA). Deionized (DI) water was employed throughout the experiments.

Partially deuterated ionic liquid, [C_2mim][OAc]-d_3, was synthesized based on a modified protocol[19] that utilized deuterated acetic acid. Briefly, 1-ethyl-3-methylimidazolium ethylsulfate was passed through a vertical column packed with an anion exchange resin (Ambersep® 900 hydroxide form) and then eluted with water. The eluted fractions having a pH > 13 were neutralized with deuterated acetic acid and the resulting product was concentrated under reduced pressure to remove excess water. The pale yellow, oily liquid was further extracted with diethyl ether and dried to constant weight under reduced pressure. The ^{1}H NMR (400 MHz, DMSO-d_6) results of the product were: δ(ppm) = 1.38 (3H, t, CH_3 in ethyl), 3.84 (3H, s, N–CH_3), 4.21 (2H, q, CH_2–N), 7.75 (1H, t, =CH–), 7.84 (1H, t, –CH=), and 9.92 (1H, s, –CH=).

2.2. Autohydrolysis and Biomass Characterization

Autohydrolysis of HP woodchips was carried out in an in-house constructed 10 L Hastelloy C276 pressure reactor, which was heated by band heaters and monitored and controlled with LabVIEW 8.6 software (National Instruments, Austin, TX). The chips (187 g) were transferred into a Teflon basket which was then inserted into the reactor. Subsequently, the reactor was sealed and placed under vacuum for 20 min. Afterwards, DI water at 1:19 (w/v) solid to liquid ratio (~3470 mL) was added into the reactor under vacuum and heated to 160 °C. The extraction was performed at 160 °C for 60 min under an autogenous equilibrium pressure of 0.717 MPa. At the completion of the experiment,

the reactor was cooled down and the liquid hydrolysate was carefully collected. The solid material (autohydrolyzed HP) was dried at 40 °C until constant moisture (less than 10% by weight), then milled with a Wiley mill (Thomas Scientific, Model # 3383-L10, Swedesboro, NJ) and passed through a 40-mesh screen (0.425 mm).

The chemical composition (glucan, xylan, arabinan, galactan, mannan, acid-soluble lignin, acid-insoluble lignin, acetyl, ash and moisture content) of all untreated and pretreated biomass was determined by following the National Renewable Energy Laboratory (NREL, Golden, CO) standard protocols TP-510-42618 (2011), TP-510-42621 (2008) and TP-510-42622 (2008). The total carbohydrates content of the liquid autohydrolyzate fraction was quantified according to NREL/TP-510-42623 (2008), where it was autoclaved with 4% sulfuric acid at 121 °C for 60 min. The concentration of monomeric sugars before and after autoclaving was determined using a PerkinElmer (Waltham, MA) high performance liquid chromatography and refractive index (HPLC-RI) detection system, fitted with a Bio-Rad Aminex HPX-87P analytical column (Richmond, CA) and a deashing guard column (Biorad, Hercules, CA), maintained at 85 °C. DI water was used as the mobile phase at a flow rate of 0.25 mL/min. The amount of lignin removed in the liquid autohydrolyzate fraction was calculated using the following equation:

$$Lignin\ (\%) = \frac{m_{lignin,HP} - m_{lignin,autohydrolyzedHP}}{m_{lignin,HP}} \qquad (1)$$

where $m_{lignin,\ HP}$ represents the oven-dry weight of lignin contained in the starting biomass, and $m_{lignin,\ autohydrolyzedHP}$ is the oven-dry weight of lignin remaining in the autohydrolyzed biomass.

2.3. Activation and Regeneration of Biomass in [C_2mim][OAc]

The moisture contents of HP and autohydrolyzed HP used in the IL-activation step were 5% and 3% (w/w on dry basis), respectively. Prior to adding the biomass, [C_2mim][OAc] was heated at 100 °C for 20 min to remove any water traces and then cooled

down to 60 °C. Approximately, 10% (w/w) *i.e.,* 40 g of biomass (HP or autohydrolyzed HP) were added to [C_2mim][OAc] (360 g) maintained at 60 °C and mechanically mixed in a 0.9 L glass reactor at 600 RPM for 3 h. At the end of the IL-activation, room temperature DI water was quickly added to the biomass-IL system as an anti-solvent and the mixture was stirred for three additional minutes. The IL-activated biomass was filtered and washed with room temperature DI water to remove any traces of IL and finally recovered by centrifugation. The sample was then dried at 40 °C. The complete removal of IL was confirmed by monitoring a characteristic infrared band of [C_2mim][OAc] ($\nu_{C=N}$ at 1565 cm^{-1}) in the regenerated biomass using a PerkinElmer Spectrum One FT-IR spectrometer (Waltham, MA).

2.4. XRD Analysis of Hybrid Poplar Cellulose Structure

Powder XRD was used to determine the impact of autohydrolysis, IL-activation, and the combination of both on cellulose structure in the resulting biomass. Each sample (control, IL-activated, autohydrolyzed, and autohydrolyzed + IL-activated HP) was mounted on a low-background quartz holder and a PANalytical Empyrean X-ray diffractometer (PANalytical Inc., Westborough, MA) with a Cu tube (λ ¼ 1.5405 Å) was used to collect the data. The radiation was generated at 40 mA and 45 kV. A step increment of 0.01° was used for measuring the scattering angle 2θ in the range 9 – 41°. Crystallinity index (CrI) of the biomass samples was determined using peak deconvolution method,[20] where the X-ray diffractograms were fitted with pseudo-Voigt function for the crystalline area and InvsPoly function for the amorphous area using OriginPro 2020 software (Northampton, MA). CrI was calculated as the percentage of total crystalline area (1-10, 110, 200, 004) over the total area as given in the equation below.

$$\text{CrI (\%)} = \frac{Peak\ area_{crystalline\ cellulose\ I\ or\ II}}{Peak\ area_{crystalline\ cellulose\ I} + Peak\ area_{crystalline\ cellulose\ II} + Peak\ area_{amorphous}} \times 100 \quad (2)$$

160 **2.5. Enzymatic Saccharification of Hybrid Poplar**

161 Enzymatic hydrolysis of the control HP, IL-activated, autohydrolyzed, and
162 autohydrolyzed + IL-activated HP was carried out in duplicate according to the NREL
163 standard protocol TP-510-42629 (2008). Briefly, 2% (w/w) of biomass sample (10 g) were
164 hydrolyzed using a mixture of multicomponent cellulases (CTec2 @ 60 FPU/g cellulose)
165 and hemicellulases (HTec2 @ 59 U), graciously provided by Novozymes (Franklinton,
166 NC). The saccharification was performed at 50 °C in a 0.9 L fermenter with constant
167 stirring (140 RPM) and a 50 mM citrate buffer at pH 5.5. The carbohydrates conversion
168 was monitored by measuring the monomeric sugar concentration in aliquots of the
169 saccharification hydrolysates. Aliquots of 1.5 mL taken at 0, 1, 2, 3, 6, 24, 48 and 72 h were
170 boiled for several minutes to denature the enzymes and centrifuged to separate the solid
171 residues. The aliquots were then filtered with a 0.45 μm nylon membrane filter
172 (MilliporeSigma, Billerica, MA) and analysed using the previously described HPLC-RI
173 system. After 72 h hydrolysis, the solid fraction was recovered from the saccharification
174 hydrolysate by centrifugation and further washed with DI water to remove the buffer and
175 enzymes. This fraction, termed as IL-lignin, was then dried at 40 °C prior to detailed
176 characterization. The total lignin content of this fraction was determined using the two-step
177 sulfuric acid hydrolysis (Klason) procedure described in NREL/TP-510-42618 (2011).
178 Ultimate analysis of IL-lignin was performed in triplicate using the Elemental Analyzer ECS4010
179 (Costech Inc., Valentia, CA) in order to measure %C and %N, whereas a high temperature
180 conversion elemental analyzer (Thermo Finnigan, Palmer, MA) was employed to measure the %O.

181 **2.6. Thermal Analysis of IL-Lignin by DSC**

182 Thermal analysis of the isolated IL-lignin was conducted using a PerkinElmer
183 (Shelton, CT) Diamond differential scanning calorimeter (DSC). The system uses two 1 g

furnaces, which allows the fastest heating and cooling rates of up to 500 °C/min and provides an improved baseline and a better resolution of heat capacity transition. In brief, approximatively 2.5 mg of IL-lignin were placed in an indium DSC pan and sealed with a lid punctured on top to allow for any volatiles to escape. Each heating cycle ranged from 0 to 250 °C at a rate of 100 °C/min, followed by a cooling cycle from 250 to 0 °C at the same rate. The end condition was set to cool the samples to 25 °C. The heating cycle was repeated three times, whereas the cooling cycle was repeated twice to eliminate any thermal history. The glass transition temperature (T_g) was determined at the midpoint of heat capacity change during the third heat flow.

2.7. 2D-NMR Spectroscopy of Biomass and IL-Lignin

A sub-sample of the starting HP chips were ground (40 mesh) then extracted in an Accelerated Solvent Extractor (ASE 350, Dionex, Sunnyvale, CA) to remove any non-structural compounds (extractives) following the NREL standard protocol TP-510-42619 (2008). Afterwards, the extractives-free HP was ball milled according to a published protocol.[21] The milled sample (40 mg) was transferred to a 5 mm (Ø) NMR tube and then 500 µL of solvent mixture composed of DMSO-d_6 and pyridine-d_5 at 4:1 (v/v) ratio were carefully introduced along the sides of the NMR tube. The sample was then sonicated for ~1 h until a gel with a homogeneous appearance was formed. The same methodology was employed to prepare an IL-lignin gel, since this fraction was sparingly soluble in common organic solvents (<0.5% w/v in ethyl acetate, methanol, DMF) even at elevated temperatures of ≥ 50 °C (8% w/v in DMSO). Two-dimensional ^{1}H-^{13}C HSQC NMR spectra of the extractives-free HP and IL-lignin samples were acquired using a Bruker AV-II (Billercia, MA) NMR spectrometer operating at 600.13 MHz. A semi-quantitative analysis was performed by integrating the correlation peaks in different regions of the

HSQC spectra with MestReNova (v14.2, Mesterlab Research, Compostela, Spain). The relative quantity of side chains involved in different inter-unit linkages (e.g., β–aryl ether) was expressed as number per 100 (syringyl + guaiacyl) aromatic units.

2.8. Small Angle Neutron Scattering (SANS) of IL-Lignin

IL-lignin was dissolved in partially deuterated [C_2mim][OAc]-d_3 by stirring at 60 °C for up to 12 h, at concentrations ranging between 1 and 7.5% (w/w). These dissolved IL-lignin solutions were syringed into assembled 1 mm path-length titanium cells for SANS studies. Small-angle neutron scattering (SANS) measurements of these samples were performed at the Bio-SANS (CG-3) instrument located in the High Flux Isotope Reactor (HFIR) facility at the Oak Ridge National Laboratory.[22] A single instrument configuration was used to acquire data over the Q-range of 0.003 to 0.85 Å^{-1}. The sample-to-detector distance of the main detector array was 15.5 m and the west wing detector was at 1.4°. The wave-vector Q is related to wavelength (λ) and scattering angle (2θ) by $Q = \frac{4\pi}{\lambda}\sin\theta$. The reduced scattering intensity profile, $I(Q)$ versus Q, was normalized to monitor counts and corrected for detector dark current, pixel sensitivity, solid angle and background scattering prior to azimuthal averaging. SANS data analysis was performed using the IRENA package implemented in the commercially available Igor Pro Software (WaveMetrics, Inc., Portland, OR) on the solvent subtracted 1D SANS profiles.[23] Curve fitting of the SANS spectra was performed using a single level Unified Fit function (eqn. 3) which consists of a Guinier exponential and a structurally limited power law function.[24, 25]

$$I(Q) = G \exp\left(-Q^2 R_g^2/3\right) + B(Q^*)^{-\alpha} \qquad (3)$$

where G and B are the scaling factors of Guinier and power-law functions of the Unified Fit function, respectively; α is the power-law exponent, R_g is the radius of gyration, and $Q^* = Q/\left[erf\left(QR_g/\sqrt{6}\right)\right]^3$.

3. Results and Discussion

3.1. Quantitative Analysis of Autohydrolysis and IL Activation of Hybrid Poplar

Our previous work[26] had demonstrated that a large amount of HP hemicellulose could be autohydrolyzed into soluble sugars, with minor degradation to lignin and cellulose, at 160 °C for 60 min. Therefore, these conditions were adopted in this study to partially extract hemicellulose from HP. During autohydrolysis of lignocellulosic biomass, the hydrolytic cleavage of hemiacetal linkages between hemicellulose polysaccharides results in the formation of acetic acid, which is turn catalyzes further depolymerization of the carbohydrates.

Table 1. Chemical Composition of Different Process Streams During the Sequential Fractionation of Hybrid Poplar (HP)

Treatment	Chemical composition (% ODW)[#]			
	Cellulose	Hemicellulose	Total lignin[†]	Ash
HP (control)[*]	47.0 (0.2)	23.6 (0.1)	25.8 (0.2)	1.1 (0.0)
Autohydrolyzed HP	55.4 (0.7)	12.5 (0.3)	27.7 (0.1)	0.3 (0.1)
Autohydrolyzed + IL-activated HP	59.6 (0.3)	9.4 (0.2)	29.1 (2.0)	0.4 (0.0)
IL-lignin	4.3 (0.0)	2.0 (0.1)	90.1 (0.0)	0.5 (0.0)

[#]Oven dry weight; [*]Extractives-free biomass; [†]Sum of acid-soluble and acid-insoluble lignin; IL – ionic liquids. Means and standard deviations (in parenthesis) are provided for $N = 3$.

The chemical composition and mass balance of the control and autohydrolyzed HP are shown in Table 1 and Figure 1. Based on the total solid weight differences between HP and autohydrolyzed HP, the mass closure after autohydrolysis was determined to be 74% (Figure 1). Sugar quantification of the liquid hydrolysate revealed that 43.6% of the HP hemicellulose were hydrolyzed and recovered from the starting material (Figure 1). A large amount of xylan (54.1%) and the majority of galactan (95.7%) and arabinan (82.7%) were extracted during this step. Small amount of glucose was also detected, which could have originated from the hydrolysis of glucuronoxylans.

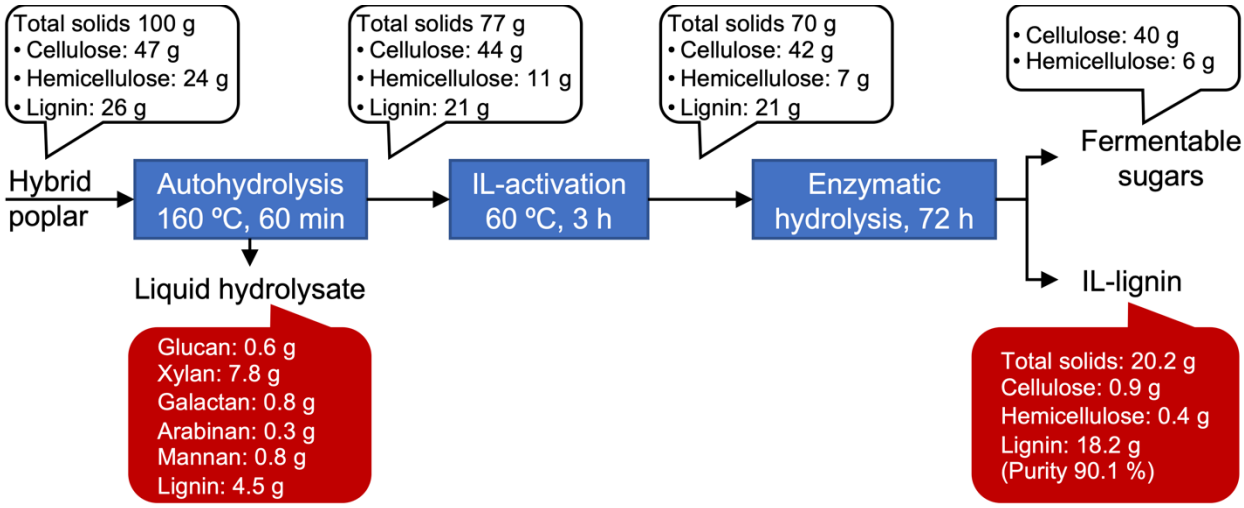

Figure 1. Quantitative analysis of the sequential fractionation process of hybrid poplar. Mass closures are based on the oven dry weight of biomass. Fractionation recoveries were: 84.6% cellulose in the enzymatic hydrolyzate, 43.6% hemicellulose in the autohydrolyzate, 23.6% hemicellulose in the enzymatic hydrolyzate, and 70.6% lignin in the enzymatic hydrolysis residues.

In addition to hemicellulose removal, the autohydrolysis step led to a significant reduction in ash content by 72%. It is worth noting that biomass with lower ash content is desirable feedstock for biorefineries since the inorganics present in biomass can cause problems with reactor equipment, such as slagging, fouling, and corrosion,[27] and in this

study, reduce the recyclability of ILs. In summary, the first step of our sequential fractionation process efficiently removed HP non-structural components, hydrolyzed a large portion of hemicellulose, and generated biomass enriched in cellulose and lignin.

In the next step, the control and autohydrolyzed HP were subjected to IL-activation in order to reduce the substrate recalcitrance. The chemical composition of resulting material is given in Table 1. During IL-activation, the hemicellulose content of the autohydrolyzed HP declined further from 12.5 to 9.4% (Table 1), demonstrating that even milder IL reactions induced hemicellulose hydrolysis. A previous study reported only 5% losses under similar conditions;[26] higher hemicellulose losses observed in this study could be attributed to the weakening of lignin-carbohydrate complexes or holocellulose interlinkages during the initial autohydrolysis step. Consequently, the autohydrolyzed + IL-activated HP had lower amount of hemicellulose and was enriched in cellulose and lignin.

3.2. Changes in Cellulose Crystallinity

The control, autohydrolyzed, and IL-activated HP exhibited diffraction patterns typical to that of cellulose Iβ (Figure 2).[20] The major peak for these three samples was at 2θ = 22.3° and secondary peaks at 2θ = 14.6° and 16.3°, corresponding to the crystallography planes of (200), (1-10) and (110), respectively. The crystallinity index (CrI) was calculated based on eqn. (2) as shown in supplemental Table S1. The CrI of the control, autohydrolyzed, and IL-activated HP was 58%, 59% and 52%, respectively. In contrast to autohydrolysis, IL-activation reduced the crystallinity of HP, which is in agreement with previous reports where IL pretreatment at 90 °C was reported to decrease the CrI of herbaceous feedstocks by up to 46%.[28] [C_2mim][OAc] is highly basic in nature and therefore, readily forms hydrogen bonds with the OH groups of cellulose resulting in swelling and subsequent loss of crystallinity when the biomass is regenerated.[29] Although

the autohydrolysis pretreatment partially removed the amorphous fractions of HP i.e., 43.6% hemicellulose and 19.5% of lignin, the resultant autohydrolyzed HP did not exhibit a significant increase in CrI. The observed increase, however small, fell within the 2-24% range predicted in previous reports for HP.[30, 31] The autohydrolyzed + IL-activated HP, on the other hand, displayed different diffraction pattern than all other treatments (Figure 2d), where the peaks corresponding to (1-10) and (110) planes shifted to 12.0° and 20.4°, respectively, indicating the appearance of cellulose II. Peak fitting using the pseudo-Voigt function (Supplemental Figure S1) showed that, this sample indeed contained a mixture of cellulose I (CrI – 25%) and cellulose II (CrI – 31%). This observation corroborates previous reports, where IL-activation of herbaceous feedstocks at comparatively higher severity (90 °C for 6 h) was shown to result in 1) decrease in cellulose crystallinity and 2) formation of transitional, lower order crystalline structure which was a mixture of cellulose I and II.[28, 29] In this study, lower order transitional state of HP crystalline cellulose was achieved even at a low severity of IL-activation (60 °C for 3h) mainly because the biomass was initially subjected to autohydrolysis. Thus, the two-step pretreatment was highly effective in introducing disorder in the crystalline structure of cellulose which would play a critical role in the subsequent enzymatic saccharification stage.

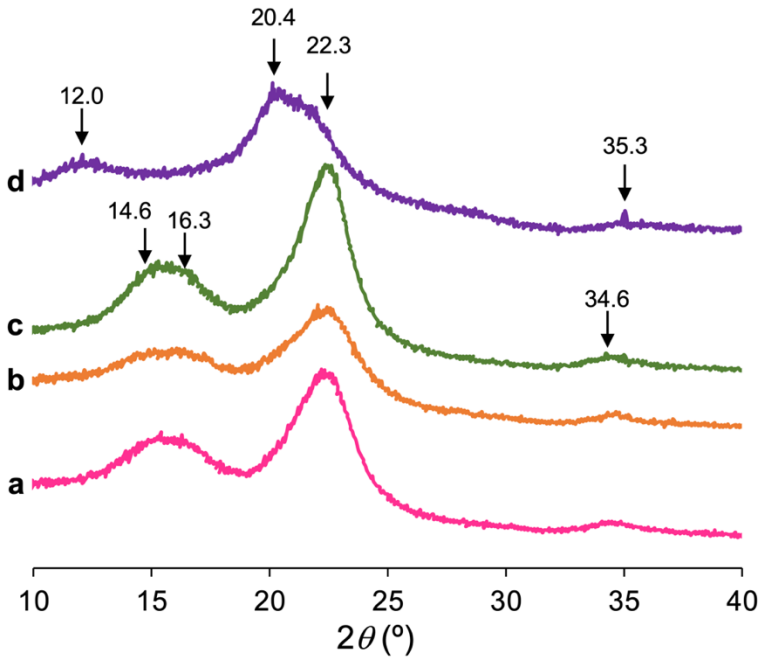

Figure 2. Powder XRD spectra of (a) untreated hybrid poplar and after (b) IL-activation, (c) autohydrolysis, (d) autohydrolysis + IL-activation.

3.3. Comparison of Saccharification Yields

The final step in our sequential fractionation process was the enzymatic saccharification that generated a fermentable sugar stream and a lignin-rich stream (termed as IL-lignin). Enzymatic saccharification was carried out for the autohydrolyzed, IL-activated, and autohydrolyzed + IL-activated HP. Of these, the two-step pretreatment was found to be more efficient in reducing the recalcitrance and improving the digestibility of HP than either autohydrolysis or IL-activation (Figure 3). Over the same reaction period, much lower cellulose conversion was observed for the autohydrolyzed HP (25%) and IL-activated HP (18%). After 72 h, only 68% of the cellulose present in the autohydrolyzed HP and 32% in the IL-activated HP were converted to glucose (Figure 3a). On the other hand, the autohydrolyzed + IL-activated HP exhibited the best performance (Figure 3a) with 87% of cellulose being hydrolyzed to glucose within 3 h. The cellulose conversion

efficiency reached a peak of 93% within 6 h, which is significantly shorter than the 24 – 72 h duration it normally takes to achieve over 90% conversion for IL-pretreated materials.[32, 33] A cellulose conversion efficiency of 91% has been reported for IL-pretreated wheat straw after 72 h,[11] whereas IL-pretreated bagasse released about 95% of glucose after 48 h.[32] Compared to these IL processes, our approach exhibited superior cellulose conversion rate.

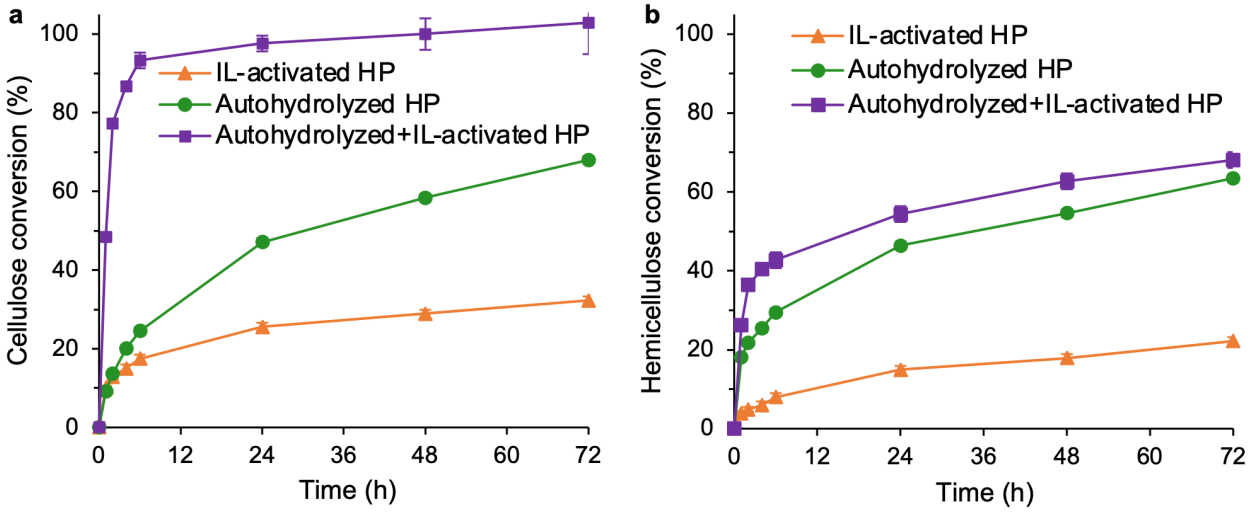

Figure 3. (a) Cellulose and (b) hemicellulose conversion (%) during enzymatic hydrolysis of pretreated hybrid poplar (HP) biomass as a function of time (error bars represent standard errors for $N = 3$).

It is worth noting that the autohydrolyzed + IL-activated HP also exhibited the best hemicellulose conversion within the treatment groups. The hemicellulose conversion efficiency was 43% after 6 h, which was higher than that of autohydrolyzed HP (30%) or IL-activated HP (8%) over the same reaction period. After 72 h, the sequentially pretreated material reached 68% hemicellulose conversion, whereas the autohydrolyzed and IL-activated HP achieved 64 and 22% conversion, respectively (Figure 3b). Studies have shown that, washing the IL-activated biomass could dramatically improve hemicellulose

conversion since the hydrolytic enzymes are more sensitive to the presence of ionic liquids, as well as to inhibitors such as humins that are generated during IL-activation.[33, 34]

The partial removal of hemicellulose and lignin during autohydrolysis and the structural changes undergone by cellulose during IL activation, together resulted in higher carbohydrate conversion of the sequentially pretreated HP. Cellulose structure has been reported to have a significant impact on enzymatic saccharification kinetics, where cellulose II was more digestible than cellulose I.[28] Accordingly, the two-step pretreated HP exhibited better digestibility due to its partially transitioned cellulose crystal structure. Although the trend in enzymatic saccharification contradicted the XRD results, where the more crystalline autohydrolyzed HP (CrI = 59%) provided better carbohydrate conversion than IL-activated HP (CrI = 52%), it also made clear that biomass digestibility is not only a function of crystallinity index but also influenced by the barrier properties of hemicellulose and lignin. Partial removal of these matrix polymers reduces the physical protection to cellulose and enhances its accessibility to cellulolytic enzymes. In summary, autohydrolysis + IL-activation resulted in significantly faster saccharification rates, gearing towards a complete conversion of cellulose and hemicellulose, thereby generating a liquid fraction rich in fermentable sugars.

3.4. Quantitative Analysis of IL-Lignin Yield and Purity

After enzymatic saccharification, the solid fraction was isolated and characterized. Chemical compositional analysis showed that it was a lignin-rich fraction with a purity of 90.1% and contained minor residues of cellulose (4.3%) and hemicellulose (2.0%) (Table 1). Ultimate analysis showed that the IL-lignin fraction contained 57.0 ± 0.1% of carbon, 35.3 ± 0.3% of oxygen, 0.2 ± 0.0% of nitrogen and an estimated 6.3 ± 0.0% of hydrogen. The elemental composition is similar to that of milled wood lignin and enzymatic

mild acidolysis lignin[35] reported in previous studies and the low nitrogen content shows that the post-enzymatic hydrolysis purification step was effective in reducing any protein contamination. Overall, the autohydrolysis + IL-activation treatment facilitated the fractionation of HP into carbohydrates- and lignin-rich fractions, with high yield and purity. The process afforded 43.6% of hemicellulose in the form of mono- and oligo-saccharides after autohydrolysis, 23.6% of hemicellulose and 84.6% of cellulose in the form of fermentable sugars after enzymatic saccharification, and finally, 70.6% of lignin in the enzymatic hydrolyzate (Figure 1). About 20% of original lignin was extracted during autohydrolysis and 10% was lost during IL activation and regeneration steps. Although the total recovery was lower than previous reports, where 82 to 91% recoveries have been reported for protic ionic liquid[7] and hot water pretreatments,[36] the quality of IL-lignin obtained in this study was higher due to conserved inter-unit linkages and lower dispersity as shown in the ensuing sections.

3.5. IL-Lignin Characterization Using 2D-HSQC NMR

Any fractionation process influences the structural properties of the isolated lignin.[36, 37] IL pretreatment was shown to cleave the inter-unit linkages, especially β-O-4, in lignin.[7, 38] Hot water pretreatment, on the other hand, was reported to significantly reduce the aromatic groups, specifically the *p*-hydroxybenzoate region, of HP lignin.[39] To assess the changes in lignin structure during our sequential fractionation process, we employed 2D-HSQC NMR to compare with the inherent properties of lignin found in untreated HP. The NMR spectra of HP (starting material) and IL-lignin (Figure 4) were divided into two regions; aromatic and side-chain. In the aromatic region of NMR spectra, *native* HP lignin showed syringyl (S), guaiacyl (G), *p*-hydroxybenzoate (P), and cinnamyl alcohol groups (Figure 4a and Table 2). As observed in Figure 4b, except for a slight reduction in oxidised

syringyl (S') groups, the signals for S, G, and P units were present in the IL-lignin, thereby demonstrating that the fractionation process did not significantly affect these aromatic units. On the other hand, cinnamyl alcohol end groups were not detected in IL-lignin (Figure 4b), which is most likely due to their cleavage during the autohydrolysis process.[39]

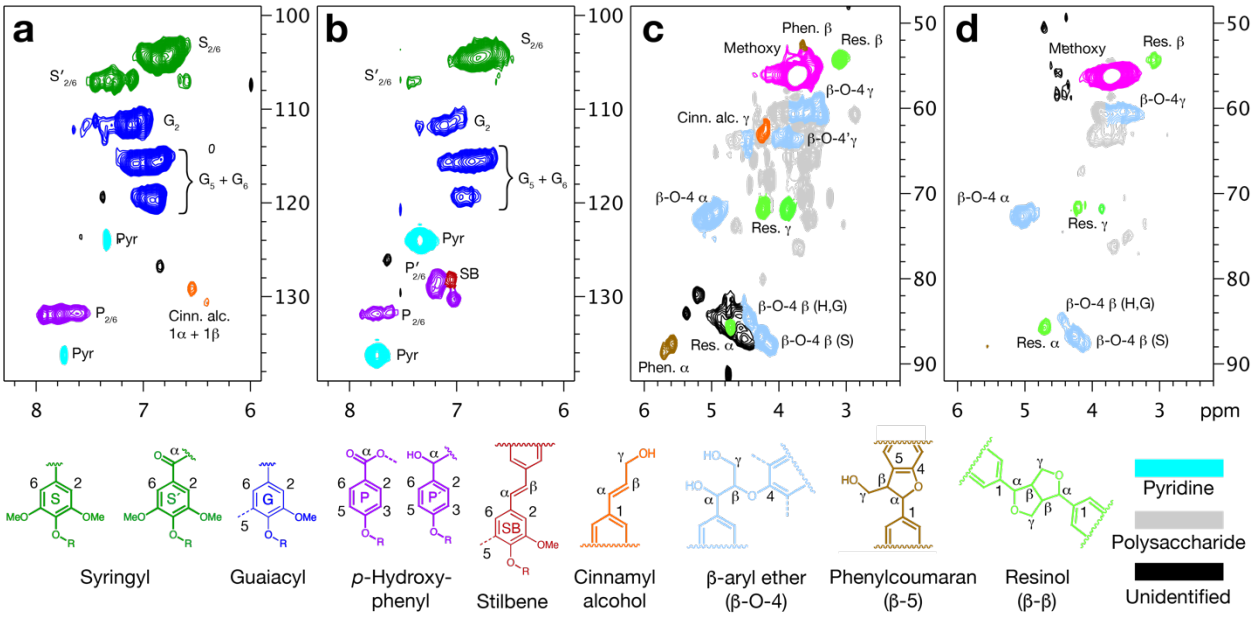

Figure 4. 2D-HSQC NMR spectra depicting the aromatic regions of (a) untreated hybrid poplar (HP), (b) IL-lignin, and the side-chain regions of (c) HP and (d) IL-lignin.

In the side chain region, there was a significant reduction in the cross-peak signals corresponding to polysaccharides in IL-lignin when compared to untreated HP, indicating its high degree of purity (Figure 4c and d). The sequential fractionation process was successful in purifying the lignin when compared to that of independently IL-activated, autohydrolyzed or cellulolytic enzyme-treated lignins reported in previous studies.[39, 40] The predominant inter-unit linkages observed in HP were β-aryl ether, phenylcoumaran, and resinol (Figure 4c); their relative quantity is reported as number per 100 aromatic (S+G) units in Table S2. The IL-lignin also displayed strong cross-peak intensities for β-aryl ether and resinol sub-structures, however, the phenylcoumaran (β-5) sub-structures were

399 significantly reduced (Figure 4d and Table S2). Previous studies have shown that ionic
400 liquid activation could degrade these structures,[41] which could result in the subsequent
401 formation of stilbenes (SB) via reverse aldol reaction[42] or *p*-hydroxyphenyl groups (P')
402 with α-OH functionality. The choice of ionic liquids has had a significant effect on the
403 structure of isolated lignin; bio-based and protic ILs have been reported to degrade the
404 principal inter-unit linkages (β–O–4′, β–β′) of regenerated lignin.[38] On the other hand,
405 autohydrolysis has been shown to increase the amount of phenylcoumaran (β-5) due to
406 recondensation or repolymerization of the solubilized lignin.[41] Our results demonstrated
407 that the β-aryl ether inter-unit linkages were reduced by only 10% in IL-lignin when
408 compared to native HP lignin (Table S2). Hence, unlike previous reports, the sequential
409 fractionation technique only caused minor degradation to IL-lignin sub-structures,
410 prevented repolymerization or condensation, as well as preserved most of the original inter-
411 unit linkages. The mild severity of the autohydrolysis and IL-activation processes has to be
412 the underlying reason for the conservation of native linkages in IL-lignin.

413 **Table 2**. **2D-HSQC NMR Assignments and Annotations for Lignin**

δ ^{13}C, ^{1}H (ppm)	**Assignment**
Aromatic region	
131.8, 7.7 131.7, 7.6	$C_{2,6}/H_{2,6}$ in P(H) benzoate
130.2, 7.0 128.5, 7.3	$C_{2,6}/H_{2,6}$ in P(H) with α-OH
127.9, 7.0	$C_{\alpha,\beta}/H_{\alpha,\beta}$ in SB
120.7, 7.5	C_6/H_6 in G with α-C=O
119.4, 6.9	C_6/H_6 in G
115.6, 7.1	$C_{3,5}/H_{3,5}$ in P(H)
115.6, 6.9	C_5/H_5 in G
112.1, 7.3	C_5/H_5 in G with 4-ether
112.0, 7.1	C_2/H_2 in G
107.1, 7.4	$C_{2,6}/H_{2.6}$ in S with α-C=O
104.3, 6.8	$C_{2,6}/H_{2.6}$ in S
Side-chain region	

87.3, 4.2	C_β/H_β in β-O-4 in S
86.8, 4.3	C_β/H_β in β-O-4 in G
85.7, 4.7	C_α/H_α in resinol (β-β')
84.7, 4.4	C_β/H_β in β-O-4 in P(H)
72.7, 5.0	C_α/H_α in β-O-4
71.6, 3.9 and 4.2	C_γ/H_γ in resinol (β-β')
62.2, 3.8 and 4.3	C_γ/H_γ in γ-acetylated β-O-4'
59.7, 3.4 – 3.7	C_γ/H_γ in β-O-4
56.2, 3.7	methoxy
54.3, 3.1	C_β/H_β in resinol (β-β')

3.6. Thermal Analysis of IL-Lignin

The thermal features of IL-lignin were analysed by DSC (Figure 5) and a glass transition temperature (T_g) of 181 °C was determined, which was higher than that of ball-milled lignin (148 °C) and organosolv lignin (135 °C) produced in-house from the same HP feedstock. The glass transition occurred within a narrow temperature range of about 20 °C, which is lower than previously reported ranges of 30 to 50 °C for technical lignins, thereby indicating a comparatively lower dispersity for the IL-lignin.[36, 37] Unfortunately, we could not substantiate this claim by measuring the molecular weight distribution, because the IL-lignin was insoluble in most organic solvents even after derivatization via acetylation or aceto-bromination. Previous studies have shown that the T_g of lignin may vary depending on the nature of the feedstock, extraction process, extraction severity, type of functional groups and intermolecular linkages.[36, 37] In general, lignins with higher degree of condensation and lower degree of methoxylation exhibited higher T_g values.[36] Preservation of the stable β-β' (resinol) sub-structures in IL-lignin (Figure 4d), along with the minor degradation of methoxylated S' groups (Figure 4b), could explain the observed higher T_g value.

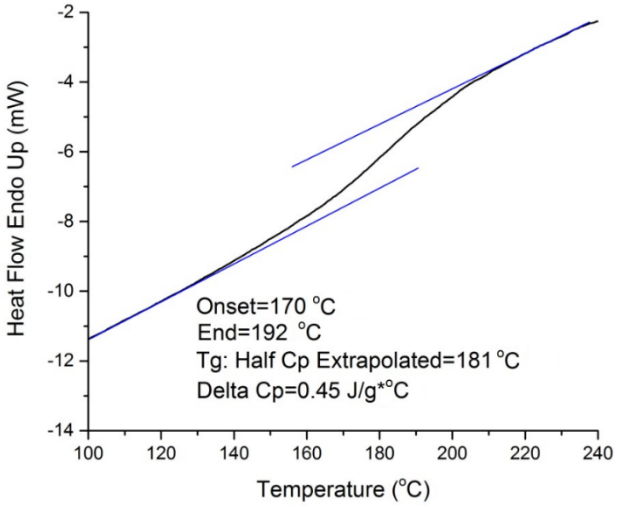

Figure 5. Differential scanning calorimetry profile of IL-lignin, isolated via sequential autohydrolysis, ionic liquid activation and enzymatic saccharification.

3.7. Physical Characterization of IL-Lignin by Neutron Scattering

Small-angle neutron scattering (SANS), a valuable technique for elucidating the structural features of hierarchical systems, was applied to investigate IL-lignin dissolved in [C_2mim][OAc]-d_3. Partially deuterated [C_2mim][OAc] was employed in order to reduce incoherent background contribution. All hydrogenated solvents, aqueous or organic, have a large incoherent background contribution to the total scattering unless their deuterated versions are used. SANS data for 7.5% (w/w) IL-lignin dissolved in [C_2mim][OAc]-d_3 displayed a linear profile on a log-log plot (Figure 6a); the slope of the linear profile represents the bulk morphology of lignin polymer. In the low-q region, a slight deviation from the linear trend is observed and therefore, the SANS data were fitted with a Unified function that consists of Guinier and power-law regimes. Although, the Unified fit function allows to extract two structural parameters, *i.e.*, the power-law exponent, α, and the radius of gyration, R_g, only the trend in the former parameter is discussed. The later parameter is

not used for interpretation because the Guinier region of IL-lignin falls in the inaccessible q-region ($Q < 0.003$ Å^{-1}).

The power-law exponent of IL-lignin in [C_2mim][OAc]-d_3 was determined to be 2.03 ± 0.04; an α of 2 indicated that IL-lignin chains conformed randomly in the given solvent. The power law exponent did not change significantly even when the IL-lignin concentration was varied from 1.0, 2.5, 5.0 to 7.5% (w/w) (Figure 6b). The fact that, solitary polymer chain conformations were observed is indicative of molecular level interactions between IL-lignin and [C_2mim][OAc]-d_3.[43] Similar molecular level interaction has been previously reported between cellulose and ILs, where the formation of electron donor-acceptor complexes was proposed to be the underlying mechanism.[44] However, the mechanism of interaction between IL-lignin and [C_2mim][OAc] is yet to be deciphered. Moreover, IL-lignin was recalcitrant to dissolution in DMSO, DMF and other molecular solvents with comparable hydrogen bond basicity (β), which indicates that further research is needed to explore this unique property of IL-lignin, its functionality and interactions with ILs.

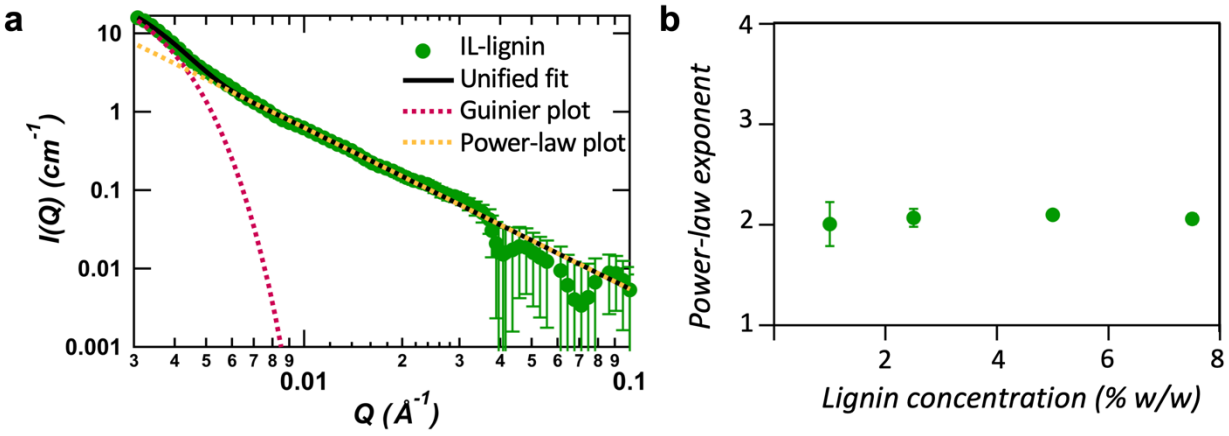

Figure 6. (a) Small-angle neutron scattering profile (green solid circles) and Unified fit (solid black line) of 7.5% IL-lignin dissolved in [C_2mim][OAc]-d_3; (b) Power law exponent (α) plotted as a function of IL-lignin concentration in [C_2mim][OAc]-d_3.

4. Conclusions

Lignocellulosic biomass was successfully fractionated into carbohydrate and lignin-rich fractions by employing a sequential autohydrolysis, mild IL-activation and enzymatic saccharification process. Approximately, 84.6% of cellulose, 67.2% of hemicellulose, and 70.6% of lignin were fractionated and isolated through this method, with a high degree of purity and minimal mass loss. The autohydrolysis step improved the accessibility of cellulose, whose crystalline structure was then transformed during the IL-activation step resulting in a significantly higher enzymatic digestibility. The sequential fractionation process also generated a lignin-enriched fraction with 90.1% purity, higher thermal stability (181 °C) and minimal degradation to inter-unit linkages which demonstrated that the proposed strategy has minimal adverse impact on lignin structure and chemistry. Thus, the sequential fractionation process resulted in better-quality lignin that could be integrated with value-added chemical and material manufacturing. Developing such processing technology that achieves the recovery of usable lignin is in line with horizontal biorefinery integration and promotion of bio-based product synthesis from primary lignocellulosic components.

Supporting Information

Figure S1- X-ray diffractograms of hybrid poplar wood powder deconvoluted using Pseudo-Voigt function and InvsPoly function in OriginPro 2020; **Table S1-** Calculation of cellulose crystallinity index (CrI) of pretreated and untreared hybrid poplar wood powder following the peak deconvolution method; **Table S2-** Semi-quantitative estimation of inter-unit linkages in hybrid poplar lignin using 2D HSQC NMR analysis.

Acknowledgments

We thank Anthony Faiia and Dr. Anna Szynkiewicz at the Stable Isotope Laboratory, Department of Earth and Planetary Sciences, in the University of Tennessee, Knoxville, for conducting the ultimate analysis of lignin sample. This work is dedicated to the friendship and memory of Dr. Luc Moens, an ionic liquid expert who made this research paper possible through his help and support over the years. We thank Ms. Lindsey Kline for her inputs in term of ionic liquid treatment and biomass regeneration. We thank Dr. Hugh O'Neill from Oak Ridge National Laboratory (ORNL) for his support with SANS experiments.

This project was primarily funded by the Southeastern Sun Grant Program and the University of Tennessee Office of Research. This research was also supported by the DOE Office of Science, Office of Biological and Environmental Research under the Genomic Science Program (FWP ERKP752). Neutron scattering research conducted at the Bio-SANS instrument, a DOE Office of Science, Office of Biological and Environmental Research resource, used resources at the High Flux Isotope Reactor, a DOE Office of Science, Scientific User Facility operated by ORNL. ONRL is managed by UT-Battelle, LLC, for the U.S. DOE under contract DE-AC05-00OR22725. The publisher, by accepting the article for publication, acknowledges that the United States Government retains a non-exclusive, paid-up, irrevocable, world-wide license to publish or reproduce the published form of this manuscript, or allow others to do so, for United States Government purposes. The U. S. Department of Energy will provide public access to these results of federally sponsored research in accordance with the DOE Public Access Plan (http://energy.gov/downloads/doe-public-access-plan).

References

1. Mosier, N.; Wyman, H.; Dale, B.; Elander, R.; Lee, Y. Y.; Holtzapple, M.; Ladisch, M., Features of promising technologies for pretreatment of lignocellulosic biomass. *Bioresour. Technol.* **2005,** *96*, 673–86, DOI: 10.1016/j.biortech.2004.06.025
2. Baruah, J.; Nath, B. K.; Sharma, R.; Kumar, S.; Deka, R. C.; Baruah, D. C.; Kalita, E., Recent trends in the pretreatment of lignocellulosic biomass for value-added products. *Front. Energy Res*. **2018**, *6*, 141, DOI: 10.3389/fenrg.2018.00141
3. Senila, L.; Senila, M.; Varaticeanu, C.; Roman, C.; Silaghi-Dumitrescu, L., Autohydrolysis pretreatment and delignification of silver fir wood to obtain fermentable sugars for bioethanol production. *Energ. Source. Part A* **2015**, *37*, 1890–1895, DOI: 10.1080/15567036.2012.658139
4. Tang, W.; Wu, X.; Huang, C.; Huang, C.; Lai, C.; Yong, Q., Enhancing enzymatic digestibility of waste wheat straw by presoaking to reduce the ash-influencing effect on autohydrolysis. *Biotechnol. Biofuels* **2019**, *12*, 222, DOI: 10.1186/s13068-019-1568-7
5. Galbe, M.; Wallberg, O., Pretreatment for biorefineries: A review of common methods for efficient utilization of lignocellulosic materials. *Biotechnol. Biofuels* **2019,** *12*, 294, DOI: 10.1186/s13068-019-1634-1
6. Reddy, P., A critical review of ionic liquids for the pretreatment of lignocellulosic biomass. *S. Afr. J. Sci.* **2015,** *111*, 9, DOI: 10.17159/sajs.2015/20150083
7. Chambon, C. L.; Chen, M.; Fennell, P. S.; Hallett, J. P., Efficient fractionation of lignin- and ash-rich agricultural residues following treatment with a low-cost protic ionic liquid. *Front. Chem*. **2019,** *7*, 246, DOI: 10.3389/fchem.2019.00246
8. Elgharbawy, A. A.; Alam, M. Z.; Moniruzzaman, M.; Goto, M., Ionic liquid pretreatment as emerging approaches for enhanced enzymatic hydrolysis of lignocellulosic biomass. *Biochem. Eng. J.* **2016,** *109*, 252–267, DOI: 10.1016/j.bej.2016.01.021
9. Brandt-Talbot, A.; Gschwend, F. J. V.; Fennell, P. S.; Lammens, T. M.; Tan, B.; Weale, J.; Hallett, J. P., An economically viable ionic liquid for the fractionation of lignocellulosic biomass. *Green Chem.* **2017,** *19*, 3078–3102, DOI: 10.1039/C7GC00705A
10. Hossain, M. M.; Aldous, L., Ionic liquids for lignin processing: Dissolution, isolation, and conversion. *Aust. J. Chem.* **2012,** *65*, 1465–1477, DOI: 10.1071/CH12324

11. da Silva, S. P. M.; Costa Lopes, A. M. D.; Roseiro, L. B.; Bogel-Łukasik, R., Novel pre-treatment and fractionation method for lignocellulosic biomass using ionic liquids. *RSC Advan.* **2013,** *3*, 16040–16050, DOI: 10.1039/C3RA43091J
12. Saha, K.; Dwibedi, P.; Ghosh, A.; Sikder, J.; Chakraborty, S.; Curcio, S., Extraction of lignin, structural characterization and bioconversion of sugarcane bagasse after ionic liquid assisted pretreatment. *3 Biotech.* **2018,** *8*, 374, DOI: 10.1007/s13205-018-1399-4
13. Labbé, N.; Kline, L. M.; Moens, L.; Kim, K.; Kim, P. C.; Hayes, D. G., Activation of lignocellulosic biomass by ionic liquid for biorefinery fractionation. *Bioresour. Technol.* **2012,** *104*, 701–707, DOI: 10.1016/j.biortech.2011.10.062
14. Shi, J.; Gladden, J. M.; Sathitsuksanoh, N.; Kambam, P.; Sandoval, L.; Mitra, D.; Zhang, S.; George, A.; Singer, S. W.; Simmons, B. A., One-pot ionic liquid pretreatment and saccharification of switchgrass. *Green Chem.* **2013,** *15*, 2579–2589, DOI: 10.1039/C3GC40545A
15. Mohtar, S. S.; Tengku Malim Busu, T. N. Z.; Md Noor, A. M.; Shaari, N.; Mat, H., An ionic liquid treatment and fractionation of cellulose, hemicellulose and lignin from oil palm empty fruit bunch. *Carbohydr. Polym.* **2017,** *166*, 291–299, DOI: 10.1016/j.carbpol.2017.02.102
16. Lara-Serrano, M.; Morales-delaRosa, S.; Campos-Martín, J. M.; Fierro, J. L. G., Fractionation of lignocellulosic biomass by selective precipitation from ionic liquid dissolution. *Appl. Sci.* **2019,** *9*, 1862, DOI: 10.3390/app9091862
17. Costa Lopes, A. M. D.; Brenner, M.; Falé, P.; Roseiro, L. B.; Bogel-Łukasik, R., Extraction and purification of phenolic compounds from lignocellulosic biomass assisted by ionic liquid, polymeric resins, and supercritical CO_2. *ACS Sustain. Chem. Eng.* **2016,** *4*, 3357–3367, DOI: 10.1021/acssuschemeng.6b00429
18. Berlin, A.; Balakshin, M., Industrial lignins: Analysis, properties, and applications. In *Bioenergy research: Advances and applications*, Gupta, V. K.; Tuohy, M. G.; Kubicek, C. P.; Saddler, J.; Xu, F., Eds. Elsevier: Amsterdam, 2014; pp 315–336, DOI: 10.1016/B978-0-444-59561-4.00018-8
19. Fukaya, Y.; Sugimoto, A.; Ohno, H., Superior solubility of polysaccharides in low viscosity, polar, and halogen-free 1,3-dialkylimidazolium formates. *Biomacromolecules* **2006,** *7*, 3295–3297, DOI: 10.1021/bm060327d

20. Park, S.; Baker, J. O.; Himmel, M. E.; Parilla, P. A.; Johnson, D. K., Cellulose crystallinity index: Measurement techniques and their impact on interpreting cellulase performance. *Biotechnol. Biofuels* **2010,** *3*, 10, DOI: 10.1186/1754-6834-3-10

21. Mansfield, S. D.; Kim, H.; Lu, F.; Ralph, J., Whole plant cell wall characterization using solution-state 2D NMR. *Nat. Protoc.* **2012,** *7*, 1579–89, DOI: 10.1038/nprot.2012.064

22. Heller, W. T.; Urban, V. S.; Lynn, G. W.; Weiss, K. L.; O'Neill, H. M., Pingali, Sai Venkatesh,; Qian, S.; Littrell, K. C.; Melnichenko, Y. B.; Buchanan, M. V.; Selby, D. L.; Wignall, G. D.; Butler, P. D.; Myles, D. A., The Bio-SANS instrument at the High Flux Isotope Reactor of Oak Ridge National Laboratory. *J. Appl. Crystallogr.* **2014,** *47*, 1238–1246, DOI: 10.1107/S1600576714011285

23. Ilavsky, J.; Jemian, P. R., IRENA: Tool suite for modeling and analysis of small angle scattering. *J. Appl. Crystallogr.* **2009,** *42*, 347–353, DOI: 10.1107/S0021889809002222

24. Beaucage, G., Approximations leading to a unified exponential/power-law approach to small-angle scattering. *J. Appl. Crystallogr.* **1995**, *28*, 717–728, DOI: 10.1107/S0021889895005292

25. Beaucage, G., Small-angle scattering from polymeric mass fractals of arbitrary mass-fractal dimension. *J. Appl. Crystallogr*. **1996**, *29*, 134–146, DOI: 10.1107/S0021889895011605

26. Moyer, P.; Kim, K.; Abdoulmoumine, N.; Chmely, S. C.; Long, B. K.; Carrier, D. J.; Labbé, N., Structural changes in lignocellulosic biomass during activation with ionic liquids comprising 3-methylimidazolium cations and carboxylate anions. *Biotechnol. Biofuels.* **2018,** *11*, 265, DOI: 10.1186/s13068-018-1263-0

27. Bryers, R. W., Fireside slagging, fouling, and high-temperature corrosion of heat-transfer surface due to impurities in steam-raising fuels. *Prog. Energy Combust. Sci.* **1996,** *22*, 29–120, DOI: 10.1016/0360-1285(95)00012-7

28. Cheng, G.; Varanasi, P.; Li, C.; Liu, H.; Melnichenko, Y. B.; Simmons, B. A.; Kent, M. S.; Singh, S., Transition of cellulose crystalline structure and surface morphology of biomass as a function of ionic liquid pretreatment and its relation to enzymatic hydrolysis. *Biomacromolecules* **2011,** *12*, 933–941, DOI: 10.1021/bm101240z

29. Zhang, J.; Wang, Y.; Zhang, L.; Zhang, R.; Liu, G.; Cheng, G., Understanding changes in cellulose crystalline structure of lignocellulosic biomass during ionic liquid pretreatment by XRD. *Bioresour. Technol.* **2014,** *151*, 402–405, DOI: 10.1016/j.biortech.2013.10.009

30. Xiao, L.-P.; Sun, Z.-J.; Shi, Z.-J.; Xu, F.; Sun, R.-C., Impact of hot compressed water pretreatment on the structural changes of woody biomass for bioethanol production. *Bioresources* **2011,** *6*, 1576–1598.

31. Yao, L.; Yang, H.; Yoo, C. G.; Pu, Y.; Meng, X.; Muchero, W.; Tusk, G. A.; Tschaplinski, T.; Ragauskas, A. J., Understanding the influences of different pretreatments on recalcitrance of *Populus* natural variants. *Bioresour. Technol.* **2018,** *265*, 75–81, DOI: 10.1016/j.biortech.2018.05.057

32. Ninomiya, K.; Inoue, K.; Aomori, Y.; Ohnishi, A.; Ogino, C.; Shimizu, N.; Takahashi, K., Characterization of fractionated biomass component and recovered ionic liquid during repeated process of cholinium ionic liquid-assisted pretreatment and fractionation. *Bioresour. Technol.* **2015,** *176*, 169–174, DOI: 10.1016/j.cej.2014.07.122

33. Kassanov, B.; Wang, J.; Fu, Y.; Chang, J., Cellulose enzymatic saccharification and preparation of 5-hydroxymethylfurfural based on bamboo hydrolysis residue separation in ionic liquids. *RSC Advan.* **2017,** *7*, 30755–30762, DOI: 10.1039/C7RA05020H

34. Bernardo, J. R.; Gírio, F. M.; Łukasik, R. M., The effect of the chemical character of ionic liquids on biomass pre-treatment and posterior enzymatic hydrolysis. *Molecules* **2019,** *24*, 808, DOI: 10.3390/molecules24040808

35. Li, J.-B.; Wu, S.-B.; Li, X.-H., Chemical structure and thermochemical properties of enzymatically acidolyzed lignins from soft and hard wood. *BioRes*. **2013**, *8*, 5120–5132.

36. Ko, J. K.; Kim, Y.; Ximenes, E.; Ladisch, M. R., Effect of liquid hot water pretreatment severity on properties of hardwood lignin and enzymatic hydrolysis of cellulose. *Biotechnol. Bioeng.* **2015,** *112*, 252–262, DOI: 10.1002/bit.25349

37. Sun, Q.; Khunsupat, R.; Akato, K.; Tao, J.; Labbé, N.; Gallego, N. C.; Bozell, J. J.; Rials, T. G.; Tuskan, G. A.; Tschaplinski, T. J.; Naskar, A. K.; Pu, Y.; Ragauskas, A. J., A study of poplar organosolv lignin after melt rheology treatment as carbon fiber precursors. *Green Chem.* **2016,** *18*, 5015–5024, DOI: 10.1039/c6gc00977h

38. Dutta, T.; Isern, N. G.; Sun, J.; Wang, E.; Hull, S.; Cort, J. R.; Simmons, B. A.; Singh, S., Survey of lignin-structure changes and depolymerization during ionic liquid pretreatment. *ACS Sustain. Chem. Eng.* **2017,** *5*, 10116–10127, DOI: 10.1021/acssuschemeng.7b02123

39. Li, M.; Cao, S.; Meng, X.; Studer, M.; Wyman, C. E.; Ragauskas, A. J.; Pu, Y., The effect of liquid hot water pretreatment on the chemical-structural alteration and the reduced

recalcitrance in poplar. *Biotechnol. Biofuels* **2017,** *10*, 237, DOI: 10.1186/s13068-017-0926-6

40. Kim, K. H.; Dutta, T.; Ralph, J.; Mansfield, S. D.; Simmons, B. A.; Singh, S., Impact of lignin polymer backbone esters on ionic liquid pretreatment of poplar. *Biotechnol. Biofuels* **2017,** *10*, 101, DOI: 10.1186/s13068-017-0784-2
41. Herbaut, M.; Zoghlami, A.; Habrant, A.; Falourd, X.; Foucat, L.; Chabbert, B.; Paës, G., Multimodal analysis of pretreated biomass species highlights generic markers of lignocellulose recalcitrance. *Biotechnol. Biofuels* **2018,** *11*, 52, DOI: 10.1186/s13068-018-1053-8
42. Balakshin, M.; Capanema, E.; Chen, C.-L.; Gracz, H. S., Elucidation of the structures of residual and dissolved pine kraft lignins using an HMQC NMR technique. *J. Agric. Food Chem.* **2003**, *51*, 6116–6127, DOI: 10.1021/jf034372d
43. Wang, H.; Gurau, G.; Pingali, S. V.; O'Neill, H. M.; Evans, B. R.; Urban, V. S.; Heller, W. T.; Rogers, R. D., Physical insight into switchgrass dissolution in ionic liquid 1-ethyl-3-methylimidazolium acetate. *ACS Sustain. Chem. Eng.* **2014,** *2*, 1264–1269, DOI: 10.1021/sc500088w
44. Cao, Y.; Zhang, R.; Cheng, T.; Guo, J.; Xian, M.; Liu, H., Imidazolium-based ionic liquids for cellulose pretreatment: Recent progresses and future perspectives. *Appl. Microbiol. Biotechnol.* **2017,** *101*, 521–532, DOI: 10.1007/s00253-016-8057-8

Table of Content graphic